Supplementary Information for:

Characterising week-long South American biomass burning plume transport and in-plume formic acid evolution using IASI measurements and chemical box model

Authors: Maria P. Velásquez-García, Richard J. Pope, Steven T. Turnock, Steve R. Arnold, David P. Moore, Ailish M. Graham, Ruth M. Doherty, John J. Remedios, and Martyn P. Chipperfield

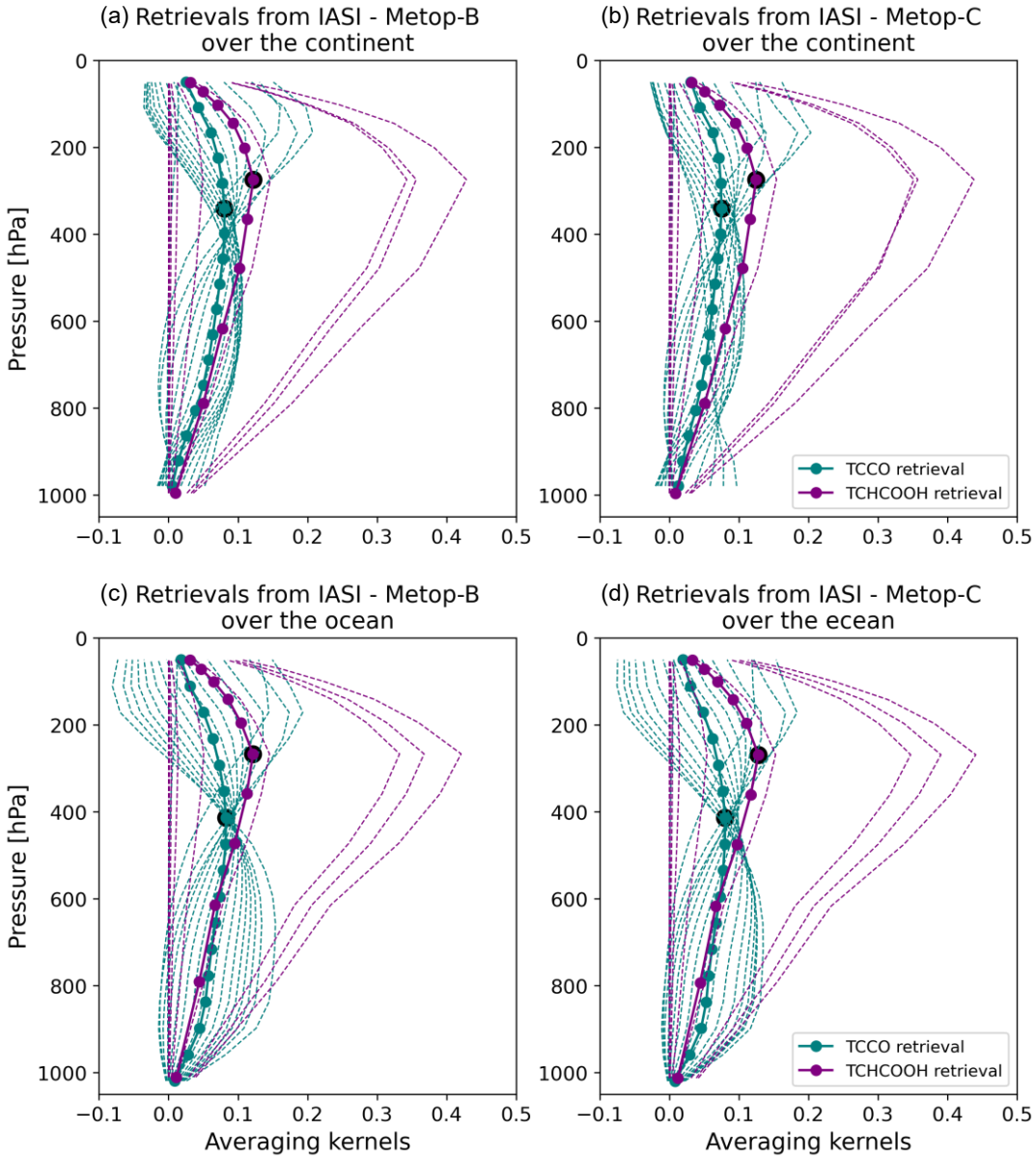


Figure S1. *Averaging kernels for the total columns CO and HCOOH products retrieved by ULIRS from IASI on board (a)(c) Metop-B and(b)(d) Metop-C over the (a)(b) South American continent and the (c)(d) Atlantic Ocean. We derived the averaging kernels from observations made from 1 to 10 September 2024 over the continent (10°S to 25°S and 50°W to 60°W) and the ocean (35°S to 20°S and 30°W to 15°W). The thick black edge in the circle marks the height of the maximum median averaging kernel.*

Text S1: ULIRS IASI HCOOH retrieval validation

This study presents the first scientific application of the University of Leicester IASI Retrieval Scheme (ULIRS) (Illingworth et al., 2011) total column HCOOH product. While a comprehensive validation suite is currently being developed by ULIRS, the novelty of this product requires an immediate, focused validation. To accomplish this, we used the TCHCOOH retrieved by the Belgian Institute for Space Aeronomy (BIRA-IASB) (Vigouroux et al., 2021) from the Fourier transform infrared (FTIR) measurement in Porto Velho (Brazil) from June to August 2019. This specific site was selected because its measurements were highly perturbed by biomass burning plumes, making it the most geographically and contextually relevant environment to evaluate the new data.

To compare the TCHCOOH products, the vertical sensitivity of the measurement retrievals should be accounted for in direct comparisons. Therefore, following Rodgers & Connor (2003), we smoothed the FTIR-retrieved profile (x_h) using the IASI-derived product averaging kernel matrix (A) and a prior profile (x_a) in equation S1, treating the FTIR measurement as "ideal".

$$\boldsymbol{x_s = x_a + \mathbf{A}(x_h - x_a)} \qquad \text{Equation S1}$$

As the BIRA-IASB profile has a finer vertical resolution, it is interpolated to the same altitudes as the ULIRS retrievals for comparison. ULIRS retrievals within 3 hours and 100 km of the FTIR measurement were used for this comparison. ULIRS retrievals were filtered for degrees of freedom (DOFs) > 0.5 and solar zenith angle < 80°.

The *a priori* for TCHCOOH retrievals was constructed from two sources: in the troposphere, the Intercontinental Chemical Transport Experiment (INTEX-B) aircraft campaign (Singh et al., 2009) and in the stratosphere, the Atmospheric Chemistry Experiment (ACE) satellite retrievals (Singh et al., 2009).

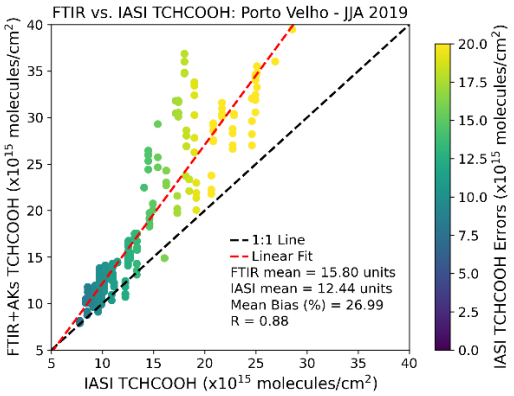


Figure S2. *Comparison between the TCHCOOH [10^{15} molecules cm^{-2}] retrieved by ULIRS (IASI, MetOp-B) and by BIRA-IASB (FTIR) for the beginning of the 2019 local fire season (June to August).*

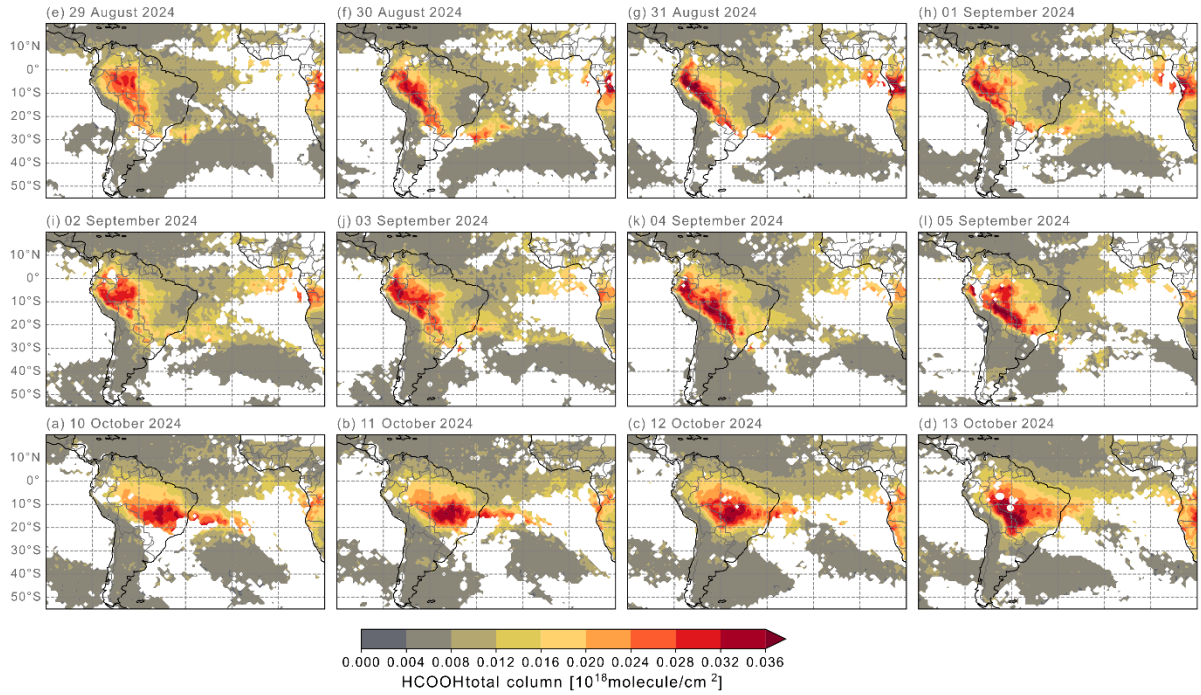


Figure S3. *Examples of biomass-burning plumes observed using total column HCOOH [10^{18} molecules cm^{-2}] retrievals on different days in (a-c) August, (d-h) September, and (i-l) October 2024 during the study period.*

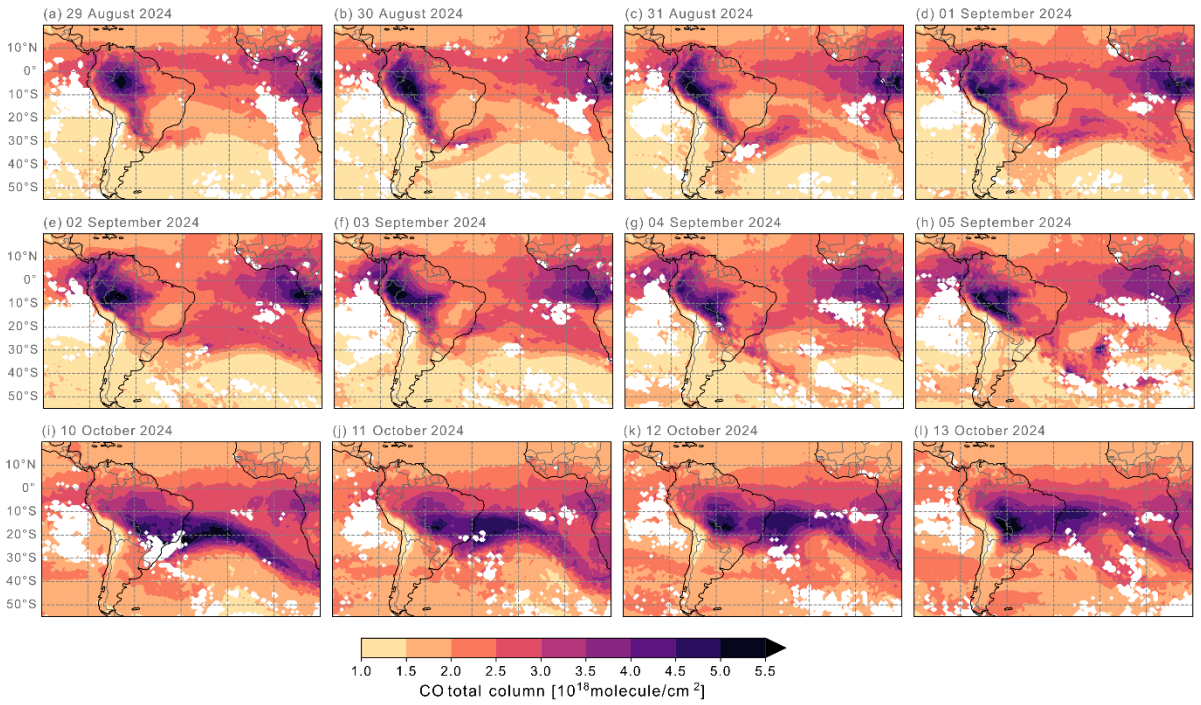


Figure S4. *Examples of biomass-burning plumes observed using total column CO [10^{18} molecules cm^{-2}] retrievals on different days in (a-c) August, (d-h) September, and (i-l) October 2024 during the study period.*

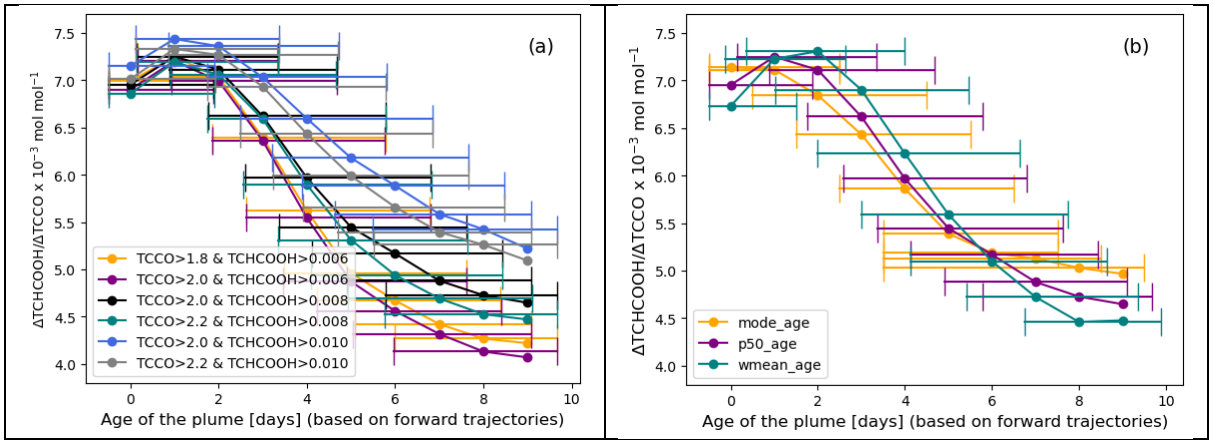


Figure S5. *Sensitivity analysis of using different (a) thresholds for TCCO and TCHCOOH for isolating the biomass burning plume and (b) average method to represent the plume age.* The horizontal lines are the interquartile range of the plumes with the same average age.

Table S2. *Initial mass mixing ratio (MMR) [kg kg^{-1}] for the UKCA box model and comparison between the control simulation and the SAMBBA-obs experiment (last column).*

Compound	Control MMR	Compound	Control MMR	Compound	Control MMR	Compound *	Control MMR	SAMBBA-obs MMR
HCHO	2.95E-09	EtOOH	1.31E-10	SO3	5.43E-21	CO	2.82E-07	2.8161E-07
O(3P)	3.38E-16	MeCHO	6.53E-10	Monoterp	1.12E-14	NO	3.96E-11	7.7015E-11
N	5.63E-38	PAN	2.37E-09	Sec_Org	9.33E-09	NO2	2.07E-10	5.1951E-10
NO3	4.1E-14	C3H8	3.02E-09	Nuc_SOL_N	1.12E-26	C2H6	9.6E-09	1.8768E-09
N2O5	8.24E-15	n-PrOOH	1.17E-11	Nuc_SOL_SU	1.23E-22	O3	1.05E-07	2.9118E-08
HO2NO2	1.04E-11	i-PrOOH	6.97E-11	Ait_SOL_N	1.18E-18	C5H8	4.5E-11	1.2972E-09
HONO2	1.88E-10	EtCHO	8.38E-12	Ait_SOL_SU	3.55E-13	C2H4	1.0E-15	2.6659E-09
H2O2	6.3E-09	Me2CO	9.05E-09	Ait_SOL_BC	3.31E-12	C3H6	1.0E-15	1.5234E-09
CH4	1.01E-06	MeCOCH2OOH	6.6E-11	Ait_SOL_OM	4.18E-11	C2H2	1.0E-15	5.0915E-10
MeOOH	3.02E-09	PPAN	4.76E-12	Acc_SOL_N	1.2E-16			
H	1.98E-21	MeONO2	2.78E-10	Acc_SOL_SU	4.22E-10	C4H10	1.0E-15	1.8941E-10
OH	1.05E-13	ISOOH	2.97E-10	Acc_SOL_BC	1.28E-09	TOLUENE	1.0E-15	9.2415E-10
HO2	4.61E-11	ISON	1.92E-09	Acc_SOL_OM	2.33E-08	BENZENE	1.0E-15	1.6180E-09
Cl	1.05E-18	MACR	2.95E-09	Acc_SOL_SS	1.04E-13	C3H8	3.02E-09	6.1092E-10
Cl2O2	2E-25	MACROOH	2.45E-09	Cor_SOL_N	2.3E-20			
ClO	8.3E-16	MPAN	2.97E-09	Cor_SOL_SU	9E-12			
OClO	2.96E-21	HACET	8.24E-09	Cor_SOL_BC	4.54E-13			
Br	3.3E-16	MGLY	2.32E-10	Cor_SOL_OM	3E-11			
BrO	6.78E-15	NALD	8.24E-10	Cor_SOL_SS	1.43E-09			
BrCl	2.62E-15	HCOOH	1.81E-09	Ait_INS_N	3.05E-17			
BrONO2	1.22E-15	MeCO3H	2.92E-09	Ait_INS_BC	3.37E-10			
N2O	4.97E-07	MeCO2H	2.65E-09	Ait_INS_OM	4.27E-09			
HCl	3.47E-14	H2	3.53E-08	Nuc_SOL_OM	9.37E-23			
HOCl	3.99E-14	MeOH	9.33E-09	Ait_SOL_NH	1.89E-12			
HBr	4.91E-13	DMS	2.67E-12	Acc_SOL_NH	1E-09			
HOBr	5.57E-14	SO2	7.53E-11	Cor_SOL_NH	3.47E-12			
ClONO2	1.72E-14	H2SO4	3.67E-17	Acc_SOL_NN	6.12E-11			
CFCl3	2.62E-09	MSA	4.33E-06	Cor_SOL_NN	1.01E-09			
CF2Cl2	3.2E-09	DMSO	6.42E-14					
MeBr	6.33E-11	NH3	4.56E-10					

HONO	6.71E-13	COS	9.99E-10					

* All compounds have the same initial mixing ratio for the control and SAMBBA-obs experiments, except for the compounds presented in the last columns.
Note: 1.0E-15 is the default mixing ratio if no other initial condition is available for the compounds used by the UKCA.

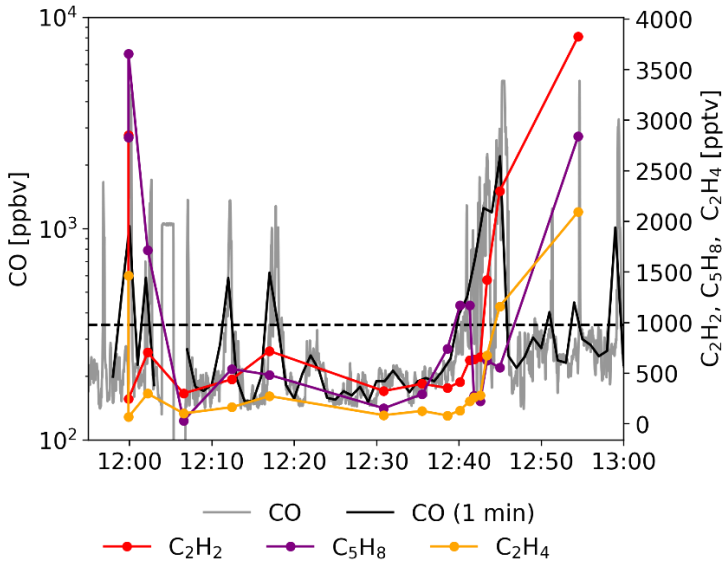


Figure S6. Time series of (left y-axis) CO [ppbv] and (right y-axis) C_2H_2, C_2H_4, and C_5H_8 [pptv] measured by the flight B737 of the South American Biomass Burning Analysis (SAMBBA) Project on September 20, 2012. The horizontal line describes the threshold of 350 ppbv, used in this study to select observations within the plume.

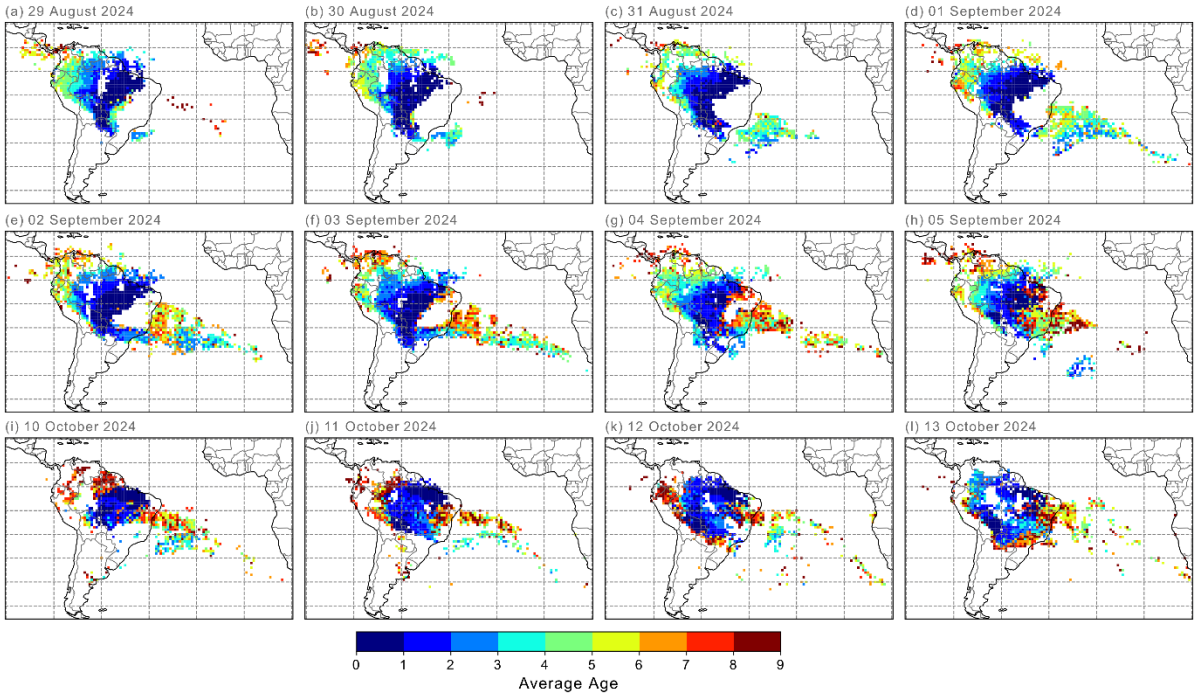


Figure S7. *Examples of age classification on biomass-burning plumes on different days in (a-c) August, (d-h) September, and (i-l) October 2024 during the study period.*

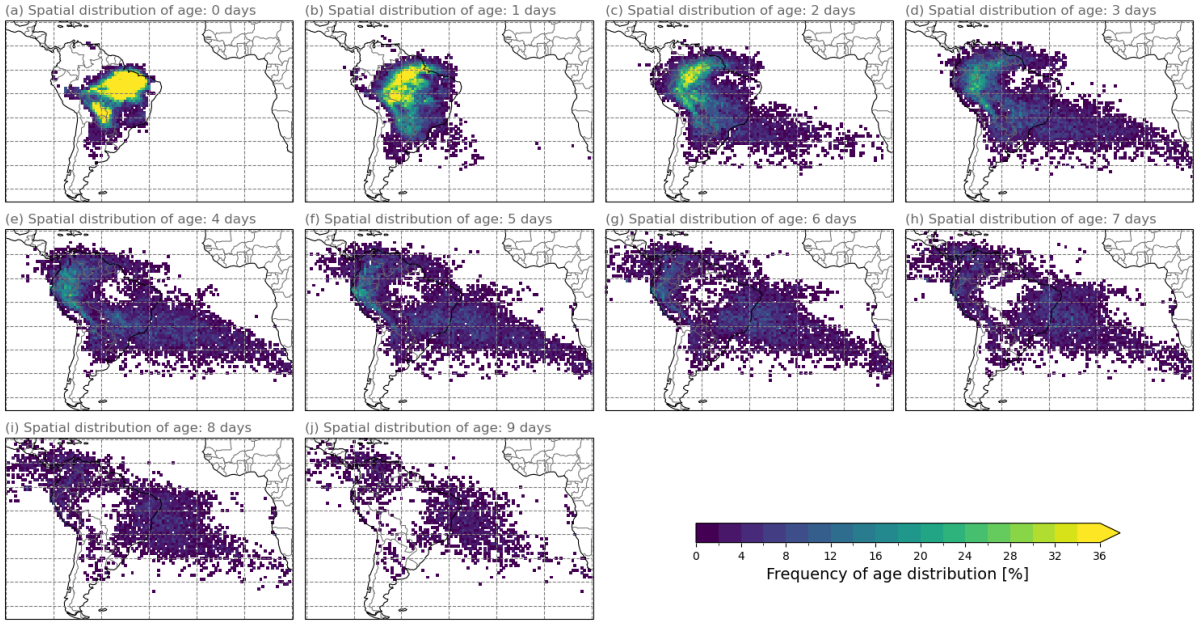


Figure S8. *Frequency distribution of plume ages for the study period August to October 2024*.

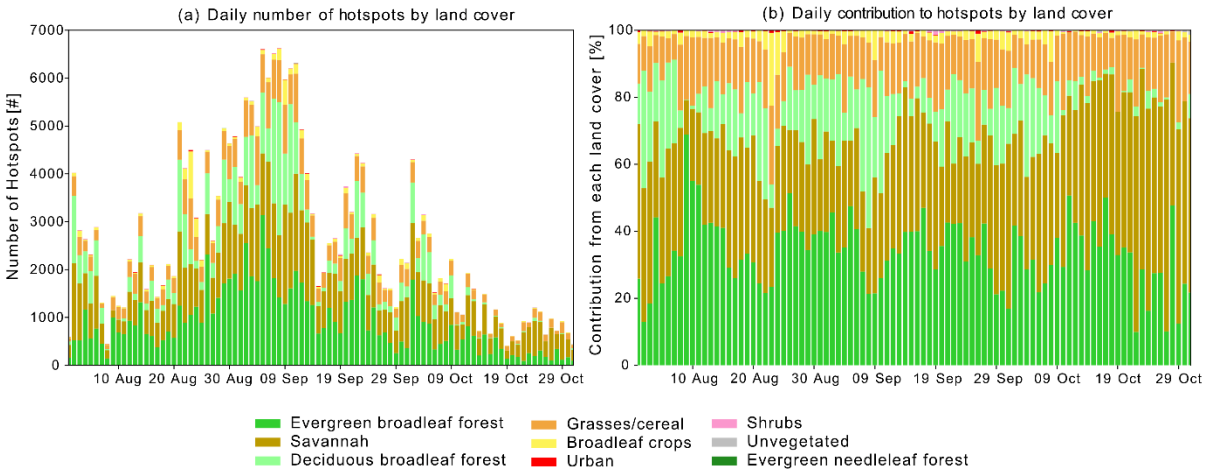


Figure S9. *Daily number of hotspots with FRP > 100MW (a) divided by dominant land cover, and (b) dominant land-cover relative contribution to daily hotspots. We calculated the dominant land cover from Myneni et al. (2002)'s land cover product in MODIS Collection 6.1 (Friedl, M., & Sulla-Menashe, D., 2022).*

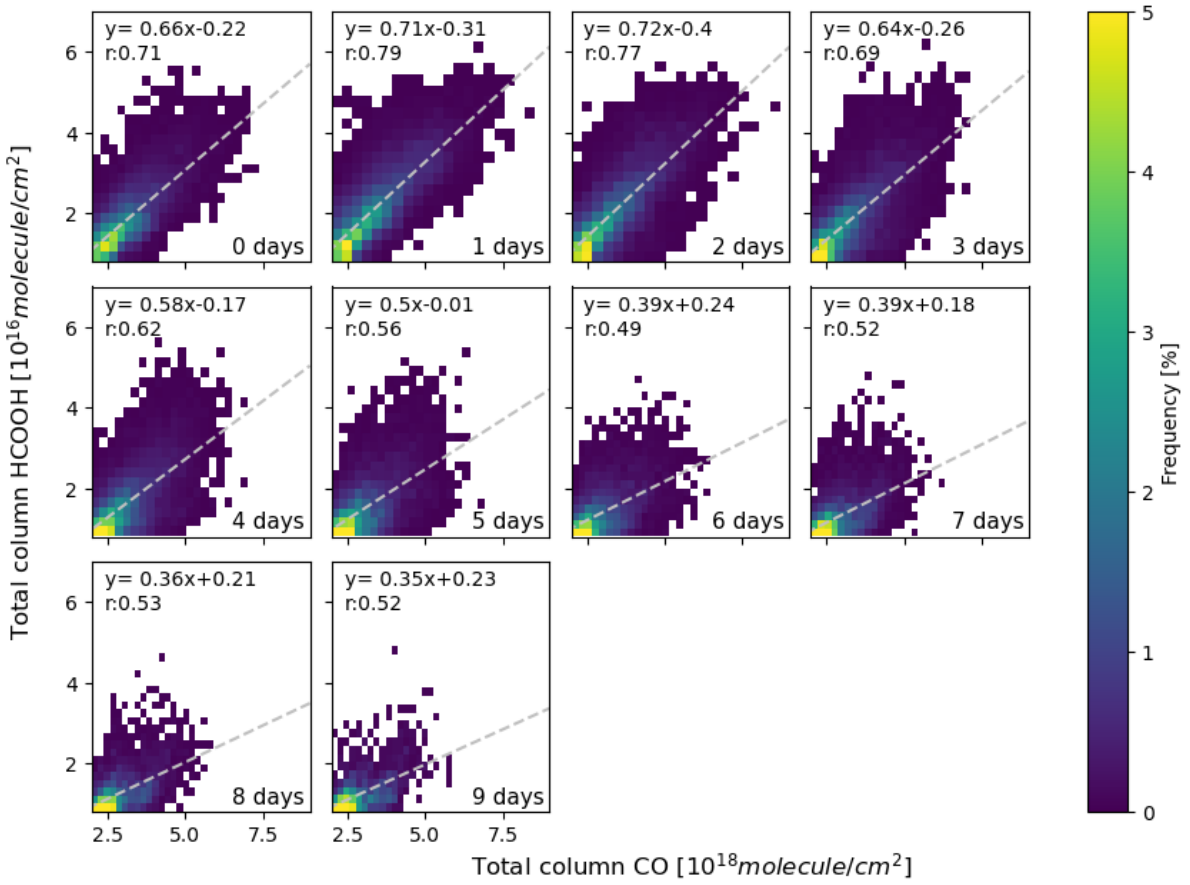


Figure S10. *Scatterplots of IASI fire-derived total column HCOOH and CO through the ageing plume on a week-long basis, including all analysed plumes (over the continental land and ocean). We used the Ordinary Least Squares regression estimator to estimate the regression coefficients.*

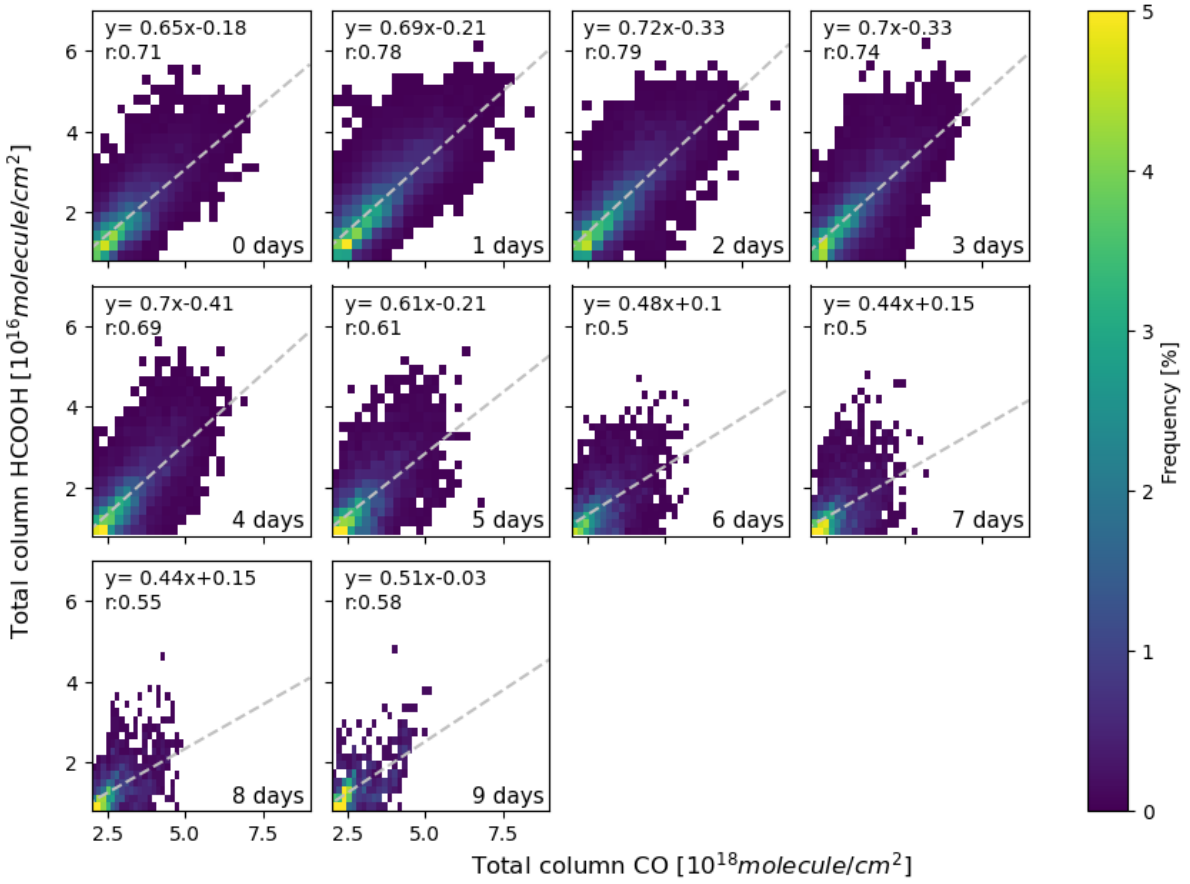


Figure S11. *Same as Fig. S9 but including only plumes over the continental land.*

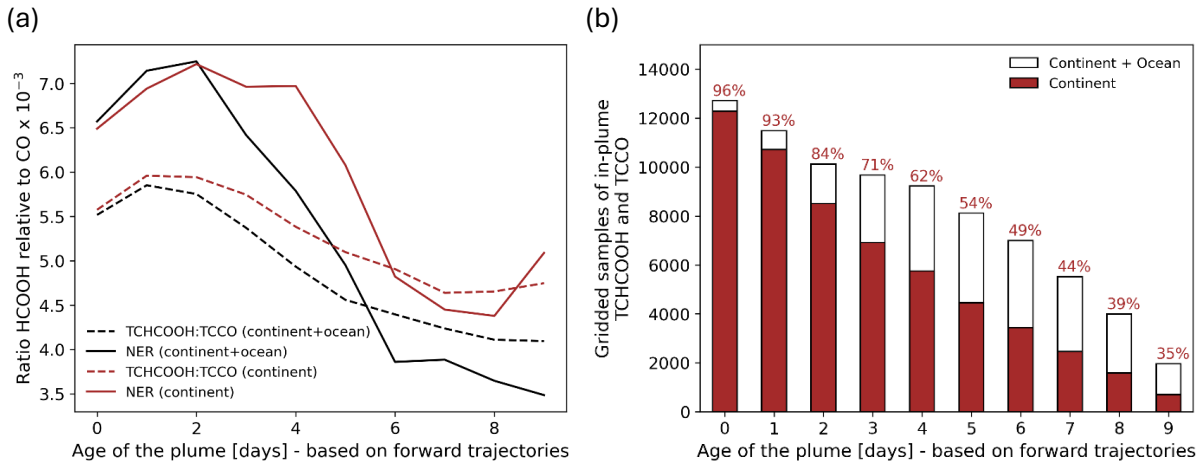


Figure S12. *(a) Comparison between the median evolution of TCHOOH:TCCO and NER$_{HCOOH}$ through the biomass burning age and (b)* gridded number of samples for continent-only plumes and the full *set of analysed plumes (including plumes over the ocean). The numbers over the bars in (b) represent the percentage of samples in the continent-only subgroup.*

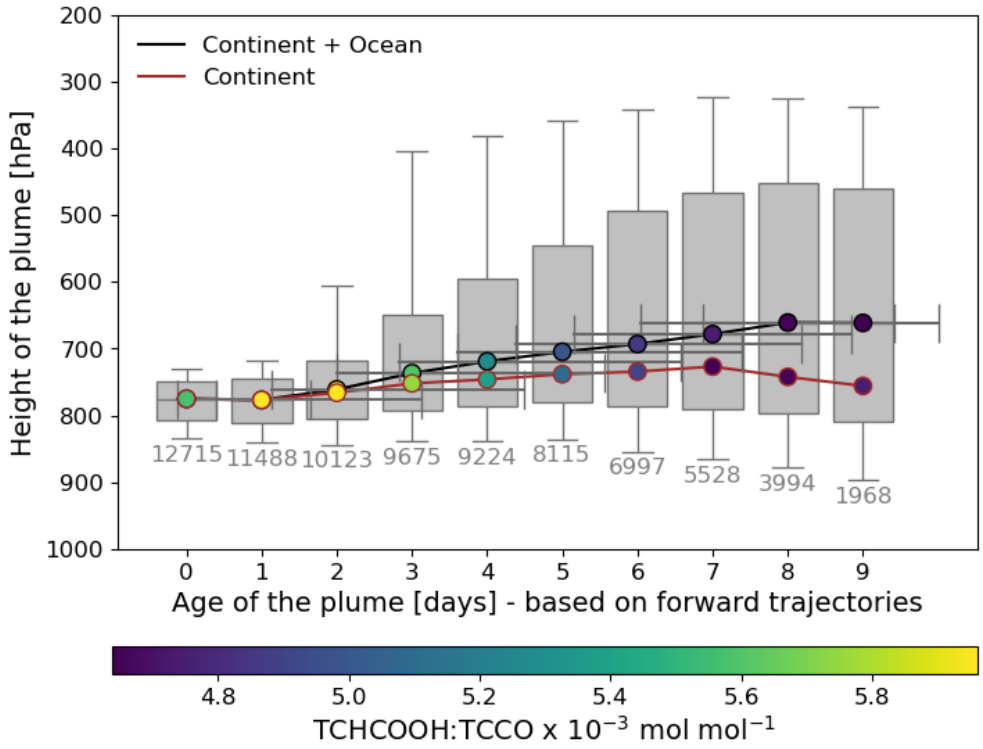


Figure S13. Box plot of plume height in the biomass burning plume versus age for the study region. The black line describes the median magnitude of all characterized plumes at each age, while the dark red line considers only plumes over continental South America (i.e., excluding plumes over the ocean). The filled circles indicate the HCOOH:CO ratio for each dataset, as shown by the colour scale.

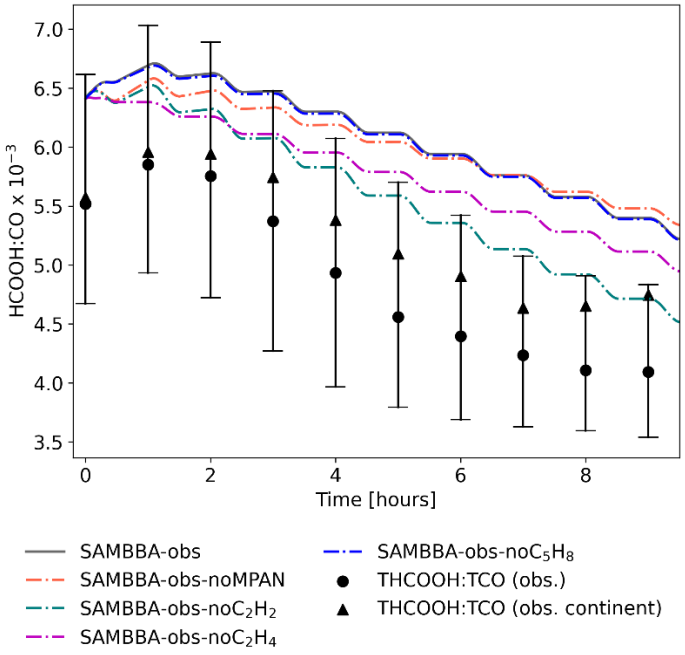


Figure S14. HCOOH:CO comparison between SAMBBA-obs-derived experiments not included in the manuscript. Similar to SAMBBA-obs-noMPAN in the manuscript, for SAMBBA-obs-

noC_2H_2, SAMBBA-obs-noC_2H_4, and SAMBBA-obs-noC_5H_8, only C_2H_2, C_2H_4, and C_5H_8, respectively, differed from SAMBBA-obs in the initial mass mixing ratio. Those compounds started at the default (1.0E-15) instead.

References

Illingworth, S. M., Remedios, J. J., Boesch, H., Moore, D. P., Sembhi, H., Dudhia, A., & Walker, J. C. (2011). ULIRS, an optimal estimation retrieval scheme for carbon monoxide using IASI spectral radiances: Sensitivity analysis, error budget and simulations. *Atmospheric Measurement Techniques*, *4*(2), 269–288. https://doi.org/10.5194/AMT-4-269-2011

Myneni, R. B., Hoffman, S., Knyazikhin, Y., Privette, J. L., Glassy, J., Tian, Y., Wang, Y., Song, X., Zhang, Y., Smith, G. R., Lotsch, A., Friedl, M., Morisette, J. T., Votava, P., Nemani, R. R., & Running, S. W. (2002). Global products of vegetation leaf area and fraction absorbed PAR from year one of MODIS data. *Remote Sensing of Environment*, *83*(1–2), 214–231. https://doi.org/10.1016/S0034-4257(02)00074-3

Rodgers, C. D., & Connor, B. J. (2003). Intercomparison of remote sounding instruments. *Journal of Geophysical Research: Atmospheres*, *108*(3). https://doi.org/10.1029/2002JD002299

Singh, H. B., Brune, W. H., Crawford, J. H., Flocke, F., & Jacob, D. J. (2009). Chemistry and transport of pollution over the Gulf of Mexico and the Pacific: Spring 2006 INTEX-B campaign overview and first results. *Atmospheric Chemistry and Physics*, *9*(7), 2301–2318. https://doi.org/10.5194/ACP-9-2301-2009

Vigouroux, C., Bauer Aquino, C. A., De Mazière, M., Gatti, L., Kumps, N., & Langerock, B. (2021). *FTIR formic acid (HCOOH) groundbased remote sensing at Porto Velho from instrument BIRA.IASB004*. Data repository of BIRA-IASB. https://doi.org/https://doi.org/10.18758/lguyweqe